IJE TRANSACTIONS C: Aspects Vol. 32, No. 12, (December 2019) 1762-1772

International Journal of Engineering

Journal Homepage: www.ije.ir

Reinforced Soil Wall Analysis under Working Stress Conditions Using a Two Phase Model with the Introduction of a New Design Parameter

A. Iraji*

Engineering Faculty of Khoy, Urmia University, Urmia, Iran

P A P E R I N F O

Paper history:
Received 07 June 2019
Received in revised form 26 October 2019
Accepted 08 November 2019

Keywords:
New Design Parameter
Non-Linear Behavior
Parametric Study
Reinforced Soil Wall Displacement
Two Phase Model
Working Stress Condition

A B S T R A C T

A previously introduced two phase model was used to assess its capability in predicting the behavior of reinforced soil walls under working stress conditions. The two phase model is a homogenization method based on the virtual work theorem. The reinforced soil medium is considered as the superposition of two continuous phases, the reinforcement and matrix phases that interact within the medium. Application of the two phase model simplifies changes in the arrangement and properties of the inclusions and decreases the computation time considerably. This approach can be used to reduce the time needed for optimization in practical applications. The introduced approach was first validated by comparison with the filed measurements. Therefore, a full-scale reinforced soil wall that has been constructed and tested under working stress condition at the Public Works Research Institute in Japan was simulated using the two phase model. A finite difference code was used to implement the two phase model and simulate the model. A nonlinear elasto-plastic law and a linearly elastic, perfectly plastic constitutive law were employed for the matrix and reinforcement phases, respectively. Then an extensive parametric study including 125 reinforced soil wall models was conducted to show the capability and strength of the introduced approach for simulation of the reinforced soil walls under working stress condition. The effect of inclusion length and stiffness, inclusion spacing, and wall height on maximum lateral displacement of the models was investigated. Eventually, a new dimensionless design parameter was introduced to achieve a simple criterion for evaluating lateral displacements.

***doi**: 10.5829/ije.2019.32.12c.09*

NOMENCLATURE

$\mathbf{D}^m$	stiffness tensor of the matrix phase	t	inclusion thickness (mm)	ρ^m	mass density of the matrix phase
$\mathbf{D}^r$	stiffness tensor of the reinforcement phase	V^{inc}	inclusion volume in one periodic layer	ρ^r	mass density of the reinforcement phase
E^{inc}	Young's modulus of the inclusion layers (kN/m^2)	V^s	soil volume in one periodic layer	$\mathbf{\Sigma}$	stress tensor of the two phase material
E^r	Young's modulus of the reinforcement phase (kN/m^2)	WL	wall length (m)	$\dot{\Sigma}_{ij}$	stress rate of the two phase material in global (1, 2, 3) space
$\mathbf{F}^m$	body force mass density applied to the matrix phase	α	angle of the inclusion layer relative to the horizon (axis 3)	$\boldsymbol{\sigma}^m$	stress tensor of the matrix phase
$\mathbf{F}^r$	body force mass density applied to the reinforcement phase	α	model constant, the PZC model	$\boldsymbol{\sigma}^r$	stress tensor of the reinforcement phase
G_0	Shear modulus, the PZC model (kN/m^2)	β_0	model constant, the PZC model	$\dot{\sigma}_{ij}^m$	stress rate of the matrix phase in global (1, 2, 3) space
H	wall height (m)	β_1	model constant, the PZC model	$\dot{\sigma}_{ij}^r$	stress rate of the reinforcement phase in global (1, 2, 3) space
H_0	plastic modulus, the PZC model	$\boldsymbol{\grave{o}}$	strain tensor of the two phase material	$\dot{\sigma}_y^r$	in-plane stress rate of the reinforcement phase in (x, y, z) coordinate system

* Corresponding Author's Email: *a.iraji@urmia.ac.ir* (A. Iraji)

Please cite this article as: A. Iraji, Reinforced Soil Wall Analysis under Working Stress Conditions Using a Two Phase Model with the Introduction of a New Design Parameter, International Journal of Engineering (IJE), IJE TRANSACTIONS C: Aspects Vol. 32, No. 12, (December 2019) 1762-1772

h	inclusion spacing (in Figure 1) (m)	$\boldsymbol{\varepsilon}^m$	strain tensor of the matrix phase	$\dot{\sigma}_z^r$	in-plane stress rate of the reinforcement phase in (x, y, z) coordinate system
$\mathbf{I}$	interaction force between the matrix and reinforcement phases	$\boldsymbol{\varepsilon}^r$	strain tensor of the reinforcement phase	σ_u^r	ultimate tensile strength of the reinforcement phase (kN/m^2)
K_0	bulk modulus, the PZC model (kN/m^2)	$\dot{\varepsilon}_{ij}^m$	strain rate of the matrix phase in (1, 2, 3) space	σ_u^{inc}	ultimate tensile strength of the inclusion in the layered model (kN/m^2)
L	inclusion length (m)	$\dot{\varepsilon}_y^r$	in-plane strain rate of the reinforcement phase in (x, y, z) coordinate system	σ_x^r	the stress perpendicular to the inclusion sheet plane
M_f	model constant, the PZC model	$\dot{\varepsilon}_z^r$	in-plane strain rate of the reinforcement phase in (x, y, z) coordinate system	σ_y^r	in-plane stress of the reinforcement phase in (x, y, z) coordinate system
M_g	slope of critical state line, the PZC model	γ	Soil unit weight (kN/m^3)	σ_z^r	in-plane stress of the reinforcement phase in (x, y, z) coordinate system
S	Inclusion spacing (in parametric study) (m)	ν^r	Poisson ratio of the reinforcement phase	X	reinforcement volume ratio

1. INTRODUCTION

Geosynthetic reinforced soil (GRS) walls show satisfactory performance against surcharge loads, asymmetric settlement and traffic and earthquake loads. GRS walls are widely used in construction projects as bridge abutments and retaining walls. The design of these structures involves stability and displacement analysis. Stability analysis can be conducted using either equilibrium or limit analysis. A GRS wall may be stable analytically; however, it may show large deformations and not satisfy serviceability. Predicting displacements of a GRS wall is always a challenge. Researchers have given special attention to experimental and numerical prediction of reinforced soil wall displacements.

Two techniques for numerical simulation of GRS walls can be employed for prediction of displacement. The first is layered, or discrete simulation in which the soil and inclusion are considered separately. To reach an optimized design for the GRS wall and satisfy deformation criteria, repeated analyses are performed using the discrete approach and the arrangement of the inclusion layers are changed for each analysis. This procedure is very time-consuming and may not be cost effective or straightforward for practical applications. The second method is the homogenization approach, which replaces reinforced soil with an equivalent homogeneous but anisotropic medium. The two phase method, as an extension of classic homogenization methods, was introduced by De Buhan and Sudret [1]. This approach is based on the virtual work theorem. It is a macroscopic description of a composite medium where the continuous matrix phase (soil) and continuous reinforcement phase (inclusion) are superposed. These phases are coincident geometrically at any point in the two phase material. A constitutive law is assigned to each of the phases. Considering strain compatibility between the phases, the global behavior of the composite can be represented by the outcome of the behavior of the two phases. The time needed to change arrangement of the inclusions during the model construction for optimal design in the two phase model is considerably low.

De Buhan and Sudret [1] used two phase model and a tensile-compressive load-carrying element for the reinforcement phase. They assigned linearly elastic, perfectly plastic constitutive laws for the reinforcement and matrix phases and assumed perfect bonding between the phases. They next added flexural behavior in addition to axial behavior for the reinforcements. Linearly elastic constitutive laws were assumed for the matrix and reinforcement phases [2]. Sudret and de Buhan [3] employed a two phase model to simulate rock-bolted tunnels and piled-raft foundations. They used the Mohr-Coulomb yield criterion and Drucker-Prager yield criterion for the matrix phases in the rock-bolted tunnel and the piled-raft foundation, respectively. Hassen and de Buhan [4, 5] simulated a piled-raft foundation subjected to vertical and lateral loading. The perfectly plastic condition accounted for the reinforcement and matrix phases. Shear, flexural and axial behaviors were considered for the inclusions. Seyedi and Farzaneh [6] introduced a two phase formulation for reinforced soil structures. They applied a relatively simple constitutive model for the matrix phase. The behavior of the reinforcement phase was regarded linear elastic-perfectly plastic. De Buhan and Hassen [7] evaluated the yield strength properties of soil medium reinforced with linear inclusions. Nguyen et al. [8] used a two phase linearly elastic continuum model associated with equations of elastodynamics to evaluate impedance of a vertically loaded piled raft foundation.

Several researchers have predicted the static behavior of GRS walls numerically and analytically. Karpurapu and Bathurst [9] predicted static behavior of GRS walls using the finite element method. They subjected GRS walls to surcharge loads and took them to the point of collapse. Moghadasnezhad [10] developed a finite element program to simulate pavements reinforced with geogrid. The results showed that using geogrid decreased vertical deformation of pavements and for strong subgrades the optimum position of geogrid in base layer is at the level of

maximum lateral displacement. Hatami and Bathurst [11] developed and validated a numerical model for the analysis of GRS walls under working stress conditions. Qhaderi et al. [12] performed several simulations to investigate the effect of soil properties, slope geometry, and reinforcement properties on the behavior of reinforced soil slopes. They validated the numerical procedure using available experimental data. Hatami and Bathurst [13] simulated four full-scale reinforced-soil segmental retaining walls numerically and evaluated the effect of backfill compaction and reinforcement type on the behavior at the end of construction and after surcharge loading. Vafaeian and Abbaszadeh [14] investigated the effect of reinforcement vertical spacing and tensile strength on the stability and failure of reinforced soil embankments subjected to surcharge loads. They found that Bishop's formula is an appropriate approach in which the effect of wall side friction and reinforcement tensile strength is taken into account. Ling and Liu [15] compared simplistic and sophisticated finite element methods for simulation of a full-scale GRS wall under static conditions. Kibria et al. [16] presented a case study and simulated it numerically. The objective of the study was to evaluate the effects of reinforcements on excessive lateral displacements of a mechanically stabilized earth wall. Shafabakhsh and Motamedi [17] studied numerically the behavior of unreinforced and reinforced pavement under different load conditions. They concluded that the position of geogrids is dependent on the base layer thickness and the ratio of elasticity modulus of asphalt to the base layer.

The two phase model proposed by Farzaneh and Iraji [18] and Iraji and Farzaneh [19] has been evaluated in the present paper to assess its capability in predicting the behavior of a full-scale reinforced soil wall under working stress conditions. A new design parameter has been introduced for evaluating lateral displacements of reinforced soil walls. The full-scale test was also simulated using the layered (discrete) approach and the results have been compared with the two phase model. In addition, given the ease of reinforced soil modeling using the two phase model, an extensive parametric study was performed to evaluate the effect of GRS wall properties on lateral wall displacement. A finite difference code, FLAC 2D, was used to simulate the models. The developed two phase model was implemented into FLAC using Fish programming. All the simulations were performed under drained conditions.

2. TWO PHASE MODEL

A brief description of the two phase model developed by Farzaneh and Iraji [18] is presented here. The nonlinear elasto-plastic constitutive model (Pastor-Zienkiewicz-Chan model, PZC) introduced by Pastor et al. [20] has been used to simulate the matrix (soil) behavior. The most important advantage of this model is its incremental nonlinear stress-strain law. Details of the PZC model can be found in Appendix A.

Sudret [21] has explained the governing equations for the equilibrium of multiphase material. He used the virtual work method, kinematics of phases and related principles. Equilibrium relations for each phase can be written as follows:

$$div\boldsymbol{\sigma}^r + \rho^r \mathbf{F}^r - \mathbf{I} = 0 \tag{1}$$

$$div\boldsymbol{\sigma}^m + \rho^m \mathbf{F}^m + \mathbf{I} = 0 \tag{2}$$

where *div* is divergence, superscripts *m* and *r* denote the matrix and reinforcement, respectively. $\boldsymbol{\sigma}^r$ and $\boldsymbol{\sigma}^m$ denote the stress tensors and $\rho^r \mathbf{F}^r$ and $\rho^m \mathbf{F}^m$ are the volume density of external body forces applied to the reinforcement and matrix phases, respectively. $\mathbf{I}$ is the interaction force between the matrix and reinforcement phases. The equilibrium relation for the two phase model can be calculated by summing the equilibrium relations for the matrix and reinforcement phases as follows:

$$div\boldsymbol{\Sigma} + \rho\mathbf{F} = 0 \tag{3}$$

where:

$$\rho\mathbf{F} = \rho^r \mathbf{F}^r + \rho^m \mathbf{F}^m \tag{4}$$

$$\boldsymbol{\Sigma} = \boldsymbol{\sigma}^r + \boldsymbol{\sigma}^m \tag{5}$$

where $\rho\mathbf{F}$ is the volume density of body force subjected to the mass of the two phase material and $\boldsymbol{\Sigma}$ is the global stress tensor of the two phase material. The total stress tensor, $\boldsymbol{\Sigma}$, is sum of the partial stresses of the matrix, $\boldsymbol{\sigma}^m$, and the reinforcement phase, $\boldsymbol{\sigma}^r$, based on the statics of the two phase medium.

The stress-strain relationship for the reinforcement and matrix phases are as follows:

$$\boldsymbol{\sigma}^r = \mathbf{D}^r \boldsymbol{\varepsilon}^r \tag{6}$$

$$\boldsymbol{\sigma}^m = \mathbf{D}^m \boldsymbol{\varepsilon}^m \tag{7}$$

where $\mathbf{D}^r$ and $\mathbf{D}^m$ are the fourth-order stiffness tensors of the reinforcement and matrix phases, respectively. $\boldsymbol{\varepsilon}^r$ and $\boldsymbol{\varepsilon}^m$ are the strain tensors of the reinforcement and matrix phases, respectively. Each phase has its own constitutive law as presented in detail by Farzaneh and Iraji [18]. The perfect bonding hypothesis was considered between the matrix and reinforcement phases as follows:

$$\boldsymbol{\varepsilon}^m = \boldsymbol{\varepsilon}^r = \boldsymbol{\epsilon} \tag{8}$$

where ϵ is the strain tensor for the composite. De Buhan and Sudret [2], Sudret and De Buhan [3], Hassen and

De Buhan [4], and De Buhan et al. [22] simulated rock-bolted tunnels and piled-raft foundations using two phase approach and perfect bonding hypothesis. Ling et al. [23], Kitsabunnarat et al. [24], Zarnani et al. [25], and Yang et al. [26] assumed perfect bonding in discrete modeling of reinforced soil structures under static and seismic loading. All the mentioned researchers concluded that the assumption of perfect bonding between the soil and inclusions in reinforced soil structure analyses has a very minor effect on the results.

Although the two phase model has some advantages over discrete analysis method, however, the main drawback of this method appears when large displacement occurs in the reinforced soil wall. Large displacements may result in local slips between the soil and reinforcements. Large displacements may be caused by big surcharge loads and strong earthquake motions or occur in high rise reinforced soil walls. Because of the perfect bonding hypothesis assumed in the two phase model, it cannot consider the slippage between the soil and reinforcements. Therefore, in the case of large displacements, the deformations predicted by the two phase model may be smaller than the observed values. In spite of perfect bonding hypothesis, there is yet an interaction and equilibrium between two phases according to Equations (1), (2), and (3).

By placing Equations (6) and (7) into Equation (5) and using Equation (8), Equation (5) can be rearranged as follows:

$$\boldsymbol{\Sigma} = \boldsymbol{\sigma}^r + \boldsymbol{\sigma}^m = \mathbf{D}^r\boldsymbol{\varepsilon}^r + \mathbf{D}^m\boldsymbol{\varepsilon}^m = \left(\mathbf{D}^r + \mathbf{D}^m\right)\dot{\boldsymbol{\varepsilon}} = \mathbf{D}\dot{\boldsymbol{\varepsilon}} \tag{9}$$

where $\mathbf{D}$ is the global stiffness tensor of the two-phase material. Note that the developed two phase model is robust enough to incorporate the internal mode of failure in which the inclusion yields, leading to large deformations and collapse of reinforced soil structures.

The inclusions were considered to be two-dimensional tensile elements. Linearly elastic perfectly-plastic behavior and the Tresca yield criterion were applied for the reinforcement phase. The reinforcement volume ratio, χ, was used to calculate macroscopic parameters (E^r, ν^r and σ_u^r) of the reinforcement phase. The reinforcement volume ratio χ is defined as the ratio of the inclusion volume (V^{inc}) to the soil volume (V^s) in one periodic layer [18, 19]:

$$\chi = \frac{V^{inc}}{V^s} = \frac{t}{h} \tag{10}$$

where t is the inclusion thickness and h is the spacing between the inclusion layers. The macroscopic properties of the reinforcement phase at a constant Poisson's ratio are calculated as follows:

$$E^r = \chi E^{inc} \tag{11}$$

$$\sigma_u^r = \chi \sigma_u^{inc} \tag{12}$$

where E^r is the corresponding macroscopic Young's modulus of the reinforcement phase in the two-phase model, E^{inc} is the Young's modulus of the inclusion layers in the layered model, σ_u^r is the corresponding macroscopic ultimate tensile strength of the reinforcement phase in the two phase model, σ_u^{inc} is the ultimate tensile strength of the inclusion in the layered model. The Tresca yield criterion is expressed as follows:

$$F = \sigma_z^r - \sigma_u^r \tag{13}$$

where σ_z^r is in-plane stress of the reinforcement phase in local Cartesian (x, y, z) system. σ_y^r is another in-plane stress of the reinforcement. Because the inclusion is regarded as a sheet under plane stress condition, σ_x^r, which is perpendicular to the inclusion sheet plane, is not considered. The mechanical parameters of the soil must not decrease because the inclusion properties already have been scaled to the soil volume (Equations (11) and (12)).

Figure 1 is a flowchart for calculating the global stress rate tensor of a reinforced medium in the two-phase scheme [18]. Two coordinate systems, global (1, 2, 3) space and the local (x, y, z) coordinate system, are defined in the two phase model. The stress rate tensor of

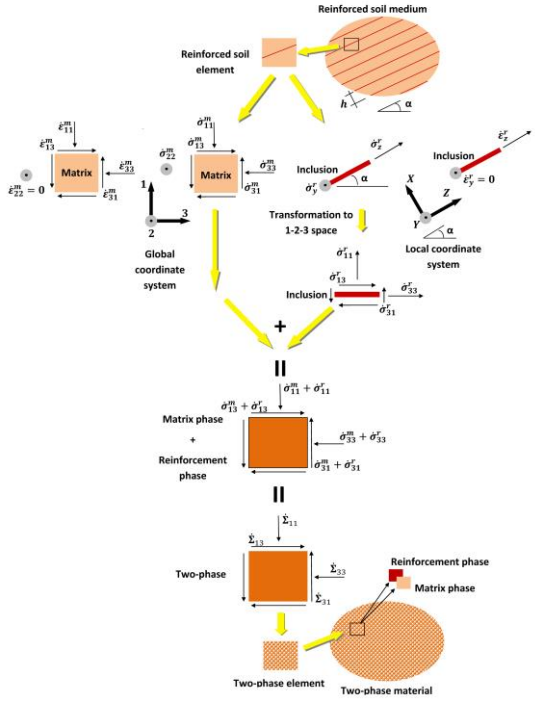

Figure 1. Flowchart for calculating global stress rate tensor of the two phase material (modified from Farzaneh and Iraji [18])

the matrix phase is defined in global (1, 2, 3) space. The stress rate tensor of the inclusion is initially defined in the local (x, y, z) coordinate system. The inclusion layer plane is set in the y-z plane. The angle of the inclusion layer relative to the horizon (axis 3) is assumed to be α. The inclusion layers are spaced equally apart (*h*). The stress rate tensor of the inclusion is transformed to global (1, 2, 3) space. The global stress rate tensor of the reinforced medium is calculated by summing the stress rate tensors of the matrix and reinforcement phases according to Equation (5).

3. TWO PHASE AND LAYERED MODELING OF A TESTED FULL-SCALE GRS WALL

To validate the proposed two phase model, a full-scale GRS wall that has been constructed in the Public Works Research Institute (PWRI) in Japan was simulated. Detailed information about the PWRI wall can be found in Tajiri et al. [27]. Figure 2 shows the configuration of the wall. The wall was constructed on a concrete foundation. It was 6.0 m in height and 5.0 m in width. Six primary geosynthetic layers with lengths of 3.5 m and five secondary geosynthetic layers with lengths of 1.0 m were used to reinforce the wall. The inclusion layers were connected to 12 concrete blocks constituting the wall facing. Each block was 50 cm in height and 35 cm in width, with the exception of the top and bottom blocks (45 and 55 cm, respectively).

3. 1. Backfill Soil Silty sand was used as the backfill. The unit weight of the soil was 16.0 kN/m^3. Three drained compression triaxial tests that had been conducted by Tajiri et al. [27] for the backfill soil were used to determine the soil model parameters. The confining pressures for the tests were 25, 50 and 100 kPa.

Table 1 shows the parameters of the soil constitutive model. The parameters were calibrated from the triaxial tests performed on the backfill soil. Two calibrated sets of the PZC model parameters for dense and loose sand samples by Pastor et al. [20] were reported here that can be compared with the values in Table 1. G_0 was taken 1.66×10^4 kPa for both of samples in Pastor et al. [20]. K_0 was taken 3.0×10^4 kPa for both of them. M_g was 1.28 for dense sand and 1.33 for loose sand. M_f was 0.72 and 0.5 for dense and loose sand samples, respectively. H_0 was 1.6×10^4 and 4.0×10^3 for dense and loose sand samples, respectively. β_0 was 2.25 for both of samples. β_1 was 0.2 for both of them.

G_0 can be derived from the initial slope of the stress-strain curve. K_0 can be derived from the isotropic compression test or by matching the initial slope of volumetric strain versus to axial strain curve. M_g is the slope of the critical state line in $p-q$ plane. It can also be determined from the curve for the stress ratio versus the shear strain or axial strain. It is approximately equal to the maximum value of stress ratio. M_f is determined using $M_f / M_g = D_r$ as a good initial approximate. D_r is relative density. α can be calculated from the curve for dilatancy versus stress ratio using Equation (4) in Appendix A. It is usually considered to be 0.45. H_0 is calculated by fitting the monotonic stress-strain curve and volumetric strain versus axial strain curve for drained tests. β_0 and β_1 are determined by matching the stress-strain curve. The recommended ranges for β_0 and β_1 are 1.0~5.0 and 0.1~0.2, respectively [20].

Figure 3 shows behavior of the backfill soil in the triaxial tests and their predicted diagrams. The soil constitutive model predicted deviatoric stress versus axial strain well. The volumetric strain variation versus axial strain was not predicted as satisfactorily as the stress-strain behavior. This prediction did not match the experimental results well.

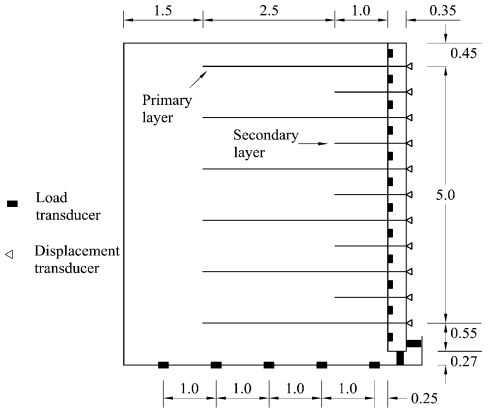

Figure 2. Configuration of PWRI wall (dimensions in m)

TABLE 1. Calibrated soil constitutive model parameters from triaxial tests

Model Parameter	Bulk modulus K_0 (kPa)	Shear modulus G_0 (kPa)	Model constant M_f	Slope of critical state line M_g	Plastic modulus H_0	Model constant β_0	Model constant β_1	Model constant α
Value	2.5×10^4	5×10^3	0.79	1.38	6×10^3	2.0	0.1	0.45

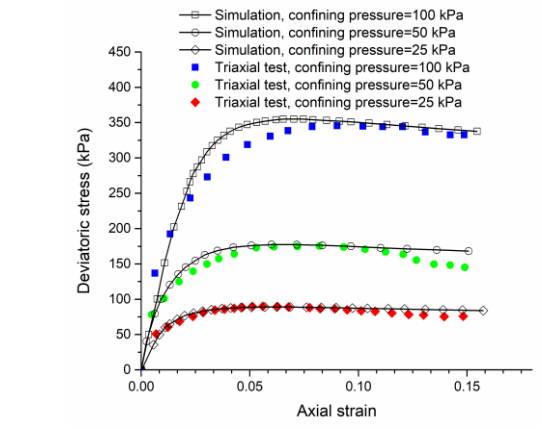

(a)

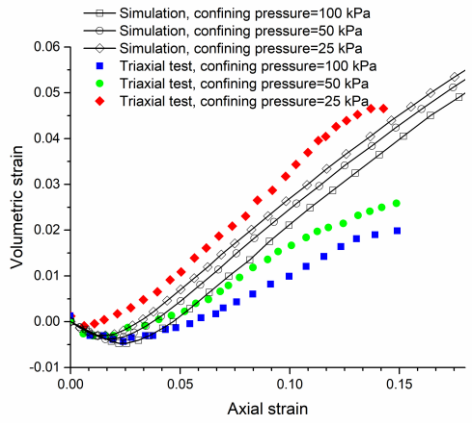

(b)

Figure 3. Comparison of triaxial tests and simulations: a) Deviatoric stress vs. axial strain; b) Volumetric strain vs. axial strain (triaxial tests from Tajiri et al. [27])

3. 2. Reinforcement A high-density polyethylene geogrid was used to reinforce the PWRI wall. Its tensile strength, measured at an axial strain of 15%, was 54 kN/m. A secant stiffness of 1436 kN/m at 0.4% strain was used for the numerical model, which was approximately the average measured value for the inclusion layers in the full-scale test. The thickness of the geogrid was not reported and was assumed to be 2.0 mm. The reinforcement volume ratio for the geogrid was calculated as χ = 0.2/100 = 0.002 for the zone reinforced by the primary layers and χ = 0.2/50 = 0.004 for the zone reinforced by the primary and secondary layers. The strength parameters of a geogrid layer were first divided by its thickness and then multiplied by the reinforcement volume ratio to calculate the reinforcement phase properties for the two phase model. The elastic modulus of the reinforcement phase was calculated as Er = 1436.0/0.002 × 0.002 = 1436.0 kN/m^2 for the zone reinforced by the primary layers and Er = 1436.0/0.002 × 0.004 = 2872.0 kN/m^2 for the zone reinforced by the primary and secondary layers. The tensile strength of the reinforcement phase was σ_u^r = 54.0/0.002 × 0.002 = 54.0 kN/m2 for the zone reinforced by the primary layers and σ_u^r = 54.0/0.002 × 0.004 = 108.0 kN/m2 for the zone reinforced by the primary and secondary layers.

3. 3. Concrete Blocks and Interfaces Linearly elastic behavior was used for the concrete blocks. The typical elastic parameters assumed for the concrete blocks were E = 2.0 × 10^6 kPa, ν = 0.17 and γ = 23 kN/m^3. Large-scale direct shear tests had been conducted for the PWRI wall to investigate the block–block and soil–block interfaces. The resulting interface friction angles for the block–block and soil–block interfaces were 19.6° and 16.5°, respectively.

3. 4. Numerical Model Numerical modeling was performed using finite difference code in FLAC 2D under the two-dimensional plane strain condition. The proposed two phase model was implemented in FLAC as a user-defined model. The forward Euler method was used for integration of the constitutive model. Figure 4 shows the finite difference mesh for the numerical model with 1920 zones for the backfill soil, 855 zones for the concrete floor and 48 zones for the facing blocks. A total of 2823 zones were used for the numerical model. The backfill soil in the model was stage constructed as for the full scale test.

3. 5. Lateral Displacements Figure 5 compares predicted lateral displacement of the PWRI wall in the two phase model with the measured displacements and the results of the layered model at different fill heights. Each concrete block was represented using 4 zones; therefore, the results are represented as a 5-point cluster. As shown, the two phase model predicted lateral displacement at fill heights of 4 m and more

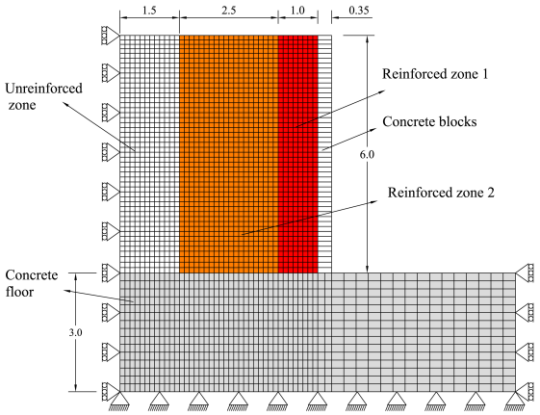

Figure 4. Finite difference mesh for PWRI wall (dimensions in meter)

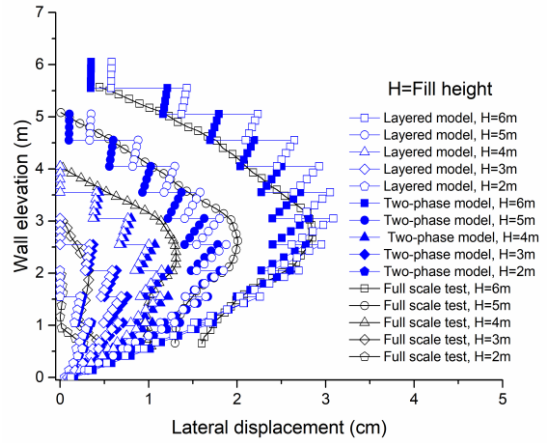

Figure 5. Predicted lateral displacement of PWRI wall for two phase model vs. measured displacement and results of layered model (Measured results from Tajiri et al. [27])

satisfactorily. The discrepancy between the maximum displacement predicted by the two phase model and the measured displacements were 7.0, 10.0 and 1.7% for fill heights of 4.0, 5.0 and 6.0 m, respectively. Good agreement can be seen between the two phase model and layered model results. Maximum discrepancy appeared at maximum displacement at a fill height of 6.0 m and was roughly 10.0%.

4. PARAMETRIC STUDY

4. 1. Model Details The effect of inclusion length, inclusion stiffness, wall height, and inclusion spacing on lateral displacement were studied extensively. The effect of facing was not addressed; therefore, the facing block was not considered and the GRS walls were assumed to be wrap-faced. 125 reinforced soil walls were simulated using the two phase model for the parametric study. Table 2 shows the details of the models. Each Category includes four sub-categories.

The yield stress of the inclusion material was 50.0 kN/m. The thickness of inclusions was assumed to be 1.0 mm. For instance the reinforcement volume ratio for

TABLE 2. Properties of reinforced soil walls in parametric study

Category 1 →	**H= 4 m** (WL = 6.6 m)	**H = 5 m** (WL = 8.2 m)	**H = 6 m** (WL = 10.0 m)	**H = 7 m** (WL = 11.6 m)
L (m) Unchanged parameters: E=6×10^5 kN/m^2 S=0.4 m γ = 16.0 kN/m^3	0.8	1.0	1.2	1.4
	1.6	1.8	2.0	2.6
	2.2	2.6	3.0	3.8
	2.8	3.4	4.0	5.0
	3.4	4.2	5.0	6.2
	4.0	5.0	6.0	7.4
	4.6	5.8	7.0	8.6
	5.2	6.6	8.0	9.8
	5.6	7.0	9.0	-
Category 2 →	**H = 4 m L= 2.8 m** (WL = 6.6 m)	**H = 5 m L= 3.4 m** (WL = 8.2 m)	**H = 6 m L= 4.0 m** (WL = 10.0 m)	**H = 7 m L= 4.8 m** (WL = 11.6 m)
E (kN/m^2) Unchanged parameters: S=0.4 m γ = 16.0 kN/m^3	2×10^5	2×10^5	2×10^5	2×10^5
	3×10^5	3×10^5	3×10^5	3×10^5
	4×10^5	4×10^5	4×10^5	4×10^5
	5×10^5	5×10^5	5×10^5	5×10^5
	6×10^5	6×10^5	6×10^5	6×10^5
	7×10^5	7×10^5	7×10^5	7×10^5
	8×10^5	8×10^5	8×10^5	8×10^5
	9×10^5	9×10^5	9×10^5	9×10^5
	1×10^6	1×10^6	1×10^6	1×10^6
	1.1×10^6	1.1×10^6	1.1×10^6	1.1×10^6
	1.2×10^6	1.2×10^6	1.2×10^6	1.2×10^6
Category 3 →	**L = 2.8 m** (WL = 6.6 m)	**L = 3.4 m** (WL = 8.2 m)	**L = 4.0 m** (WL = 10.0 m)	**L = 4.8 m** (WL = 11.6 m)
H (m) Unchanged parameters: E=6×10^5 kN/m^2 S=0.4 m γ = 16.0 kN/m^3	2.0	2.4	2.4	3.4
	3.2	3.6	3.0	4.6
	4.4	4.8	3.6	5.8
	5.6	6.0	4.8	7.0
	6.8	7.2	6.0	8.2
	8.0	8.4	7.2	9.4
	-	-	8.4	10.6
	-	-	9.6	11.8
	-	-	10.8	-
Category 4 →	**H = 4 m L= 2.8 m** (WL = 6.6 m)	**H = 5 m L= 3.4 m** (WL = 8.2 m)	**H = 6 m L= 4.0 m** (WL = 10.0 m)	**H = 7 m L= 4.8 m** (WL = 11.6 m)
S (m) Unchanged parameters: E=6×10^5 kN/m^2 γ = 16.0 kN/m^3	0.2	0.2	0.2	0.2
	0.4	0.4	0.4	0.4
	0.6	0.6	0.6	0.6
	0.8	0.8	0.8	0.8
	1.0	1.0	1.0	1.0
	1.2	1.2	1.2	1.2

Note: H = Wall height; WL = Wall length; L = Inclusion length; E = Elastic modulus of inclusion; γ = Unit weight of soil; S = Reinforcement spacing

the models with the inclusion spacing of 0.4 m was calculated as χ = 0.1/40.0 = 0.0025. The tensile strength of the reinforcement phase for these models was σ_u^r = 50.0/0.001 × 0.0025 = 125.0 kN/m^2. The elastic modulus of the reinforcement phase varied for the models. The soil used for all models was the same as that used for the PWRI project. Therefore, the same PZC model parameters were used for the parametric study.

4. 2. Numerical Model Numerical modeling in the parametric study was similar to that for the PWRI model. The soil in the model was constructed in stage and the thickness of the soil layer lifts at each stage was assumed 20 cm. FHWA [28] recommends that the lift thickness for loose backfill should not be greater than 30 cm.

4. 3. Results and Discussion In addition to the usual GRS wall parameters, a new dimensionless design parameter was introduced to evaluate its effect on lateral displacement. The dimensionless parameter is EL/SγH in which E is the elastic modulus of the inclusion, L is the inclusion length, S is the spacing between the inclusion layers, γ is the unit weight of the soil and H is the wall height.

Figure 6 shows the normalized maximum lateral displacement of models in categories 1, 2, 3 and 4. The normalized maximum lateral displacement versus *L/H*, elastic modulus of the inclusion layer, wall height and inclusion spacing are shown.

Figure 6a shows that the normalized maximum lateral displacement increased suddenly at *L/H* values smaller than 0.5. This threshold increased with an increase in the wall height of the model such that the value for the model at *H* = 7 m was 0.6. Therefore, the limit for *L/H* = 0.6 can be generalized for GRS walls of up to 7.0 m in wall height. This observation for L/H is consistent with the value recommended by the NCMA [29] of 0.6. The FHWA [28] and NCMA [29] recommend 0.7 and 0.6 as the minimum L/H to satisfy the internal and external stability and to control lateral displacement. Although L/H values of less than 0.6 are sufficient to control lateral displacement for models at H

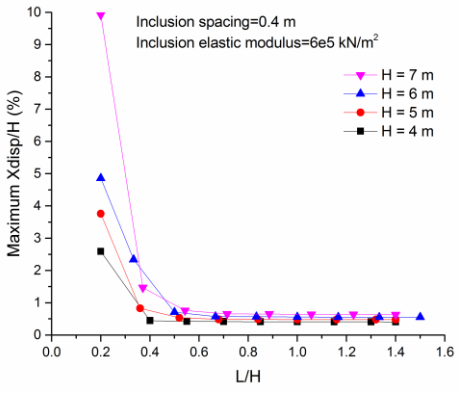

(a)

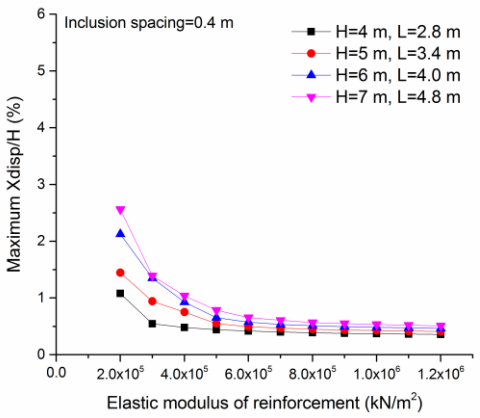

(b)

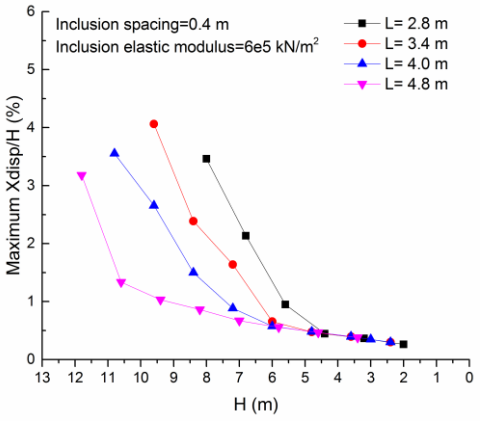

(c)

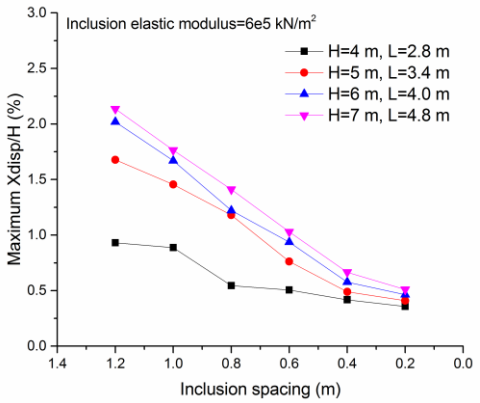

(d)

Figure 6. Normalized maximum lateral displacement of GRS walls versus: a) *L/H* for walls with different heights in category 1; b) elastic modulus of inclusion for walls of different heights and inclusion lengths in category 2; c) height for walls with different inclusion lengths in category 3; d) inclusion spacing for walls of different heights and inclusion lengths in category 4

= 4 and 5 m, the values recommended by the FHWA [28] and NCMA [29] satisfy the requirements for the H = 6 and 7 m as well. No clear critical values for the elastic modulus of the inclusion layer and its spacing can be seen in Figures 6b and 6d. Figure 6c shows that an increase in *H* increased the maximum lateral displacement significantly in the models with shorter inclusion lengths. In contrast, the model with the longest inclusion length (4.8 m) showed small lateral displacements up to the elevation of 10.8 m.

If *EL/SγH* for the horizontal axis in Figure 6 is replaced, it becomes Figure 7, in which the diagrams are aggregated and produce a more convenient interpretation. Note that not all data sets were displayed in this figure to prevent the figure from becoming so messy. Half of the data sets were removed in such a way that the overall trend of the graphs was not disturbed.

The normalized maximum lateral displacement of half of the models versus *EL/SγH* is shown in Figure 7. The NCMA [30] and PWRC [31] recommend the allowable verticality (Δx/H) of 3.5% for segmental reinforced soil walls and 3% for all types of reinforced soil walls, respectively. For instance, a value of 1% verticality is an equivalent rotation of 10 mm/m of the wall height. If we assume an allowable verticality of 2% here, it will be equivalent to normalized maximum lateral displacement of 1%. It can be concluded that normalized maximum lateral displacement can be held at under 1% by limiting the value of *EL/SγH* to 5×10^4 or more. This can be seen in Figure 7. This figure gives an appropriate evaluation of maximum lateral displacement in terms of *EL/SγH*. If the value of *EL/SγH* is held at greater than 5×10^4, the normalized maximum lateral displacement will not be greater than 1%.

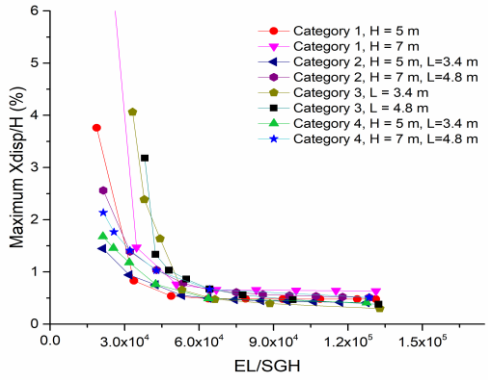

Figure 7. Normalized maximum lateral displacement of wall models versus *EL/SGH, (G=Gamma or γ)*

5. CONCLUSION

A previously introduced two phase model was used to assess its capability in simulating geosynthetic reinforced soil walls in different arrangements and under working load conditions.

A tested full scale reinforced soil wall under working stress conditions was used to validate the numerical approach. An extensive parametric study for wrapped-face reinforced soil walls was performed.

The main advantages of the two phase model are that discrete modeling of the soil and inclusions and defining a contact model between them is not needed.

It is not necessary to change the inclusion spacing and it can be addressed only by changing the reinforcement phase parameters to achieve optimal design. As tested the time required for two phase model simulation is about 60 to 65% of that of the corresponding layered simulation.

The effect of inclusion length to wall height ratio (*L/H*), inclusion elastic modulus (*E*), wall height (*H*), and inclusion spacing (*S*) were studied on the normalized lateral displacement. The critical *L/H* calculated by the two phase model was about 0.6, which is consistent with the value recommended by the NCMA [29]. The study shows that this limitation can be decreased for walls with shorter heights. The effect of a change in *H* on lateral displacement is considerable. A linear increase in lateral displacement was observed when inclusion spacing increased. The study showed that the lateral displacement for models with short inclusion lengths and greater wall heights increased remarkably. It was shown that lateral displacement can be controlled using a longer length (e.g. *L* = 4.8 m) for inclusions at greater wall heights.

Dimensionless design parameter *EL/SγH* was introduced to achieve a more simple and general criterion for evaluating lateral displacement. Lateral displacement was surveyed for different *EL/SγH* in which *E*, *L*, *S* and *H* were changed to capture all possible values for *EL/SγH*. A threshold value for *EL/SγH* of 5×10^4 was introduced for model, after which lateral displacement increased considerably. The normalized maximum lateral displacement for *EL/SγH* values greater than 5×10^4 can be held under 1%.

6. APPENDIX A: PZC MODEL

The relation between the increments of stress and strain for a material is expressed as follows:

$$\dot{\boldsymbol{\sigma}} = \mathbf{D}^{ep} : \dot{\boldsymbol{\varepsilon}} \tag{1}$$

where $\dot{\boldsymbol{\sigma}}$ is the stress rate; $\dot{\boldsymbol{\varepsilon}}$ is the strain rate; and $\mathbf{D}^{ep}$ is the elasto-plastic tensor. The elasto-plastic tensor for generalized plasticity is defined as follows:

$$\mathbf{D}^{ep} = \mathbf{D}^{ep} - \frac{\mathbf{D}^{e} : \mathbf{n}_{gL} : \mathbf{n}^{T} : \mathbf{D}^{e}}{H_L + \mathbf{n}^{T} : \mathbf{D}^{e} : \mathbf{n}_{gL}} \tag{2}$$

where $\mathbf{D}^e$ is the elastic stiffness tensor, $\mathbf{n}$ is the loading direction vector; $\mathbf{n}_{gL}$ is the plastic flow direction vector under loading; and H_L is the plastic modulus for loading. Shear and bulk moduli are expressed as follows:

$$G = G_0\left(\frac{p}{p_a}\right)^{0.5},\ K = K_0\left(\frac{p}{p_a}\right)^{0.5} \quad (3a, 3b)$$

where G_0 and K_0 are the shear and bulk modulus values, respectively; $p=I_1/3$; I_1 is the first stress invariant; and p_a (atmospheric pressure)= 101.325 kPa. The stress-dilatancy relationship is defined as follows:

$$d_g = \frac{d\varepsilon_v^p}{d\varepsilon_s^p} = (1+\alpha)(M_g - \eta) \quad (4)$$

where $d\varepsilon_v^p$ is the incremental plastic volumetric strain; $d\varepsilon_s^p$ is the incremental plastic deviatoric strain; M_g is the slope of the critical state line on the *p*-*q* plane; η *(=q/p)* is the stress ratio; and α is a model parameter. The gradient vectors for yield and potential surfaces are called the loading direction vector (**n**), and plastic flow direction vector ($\mathbf{n}_g$), respectively. These vectors are not the same in non-associated soils and defined as follows:

$$\mathbf{n} = \left(\frac{\partial f}{\partial p}, \frac{\partial f}{\partial q}, \frac{\partial f}{\partial \theta}\right)^T = \left(d_f, 1, -qM_f \cos 3\theta / 2\right)^T \quad (5)$$

$$\mathbf{n}_{gL} = \left(\frac{\partial g}{\partial p}, \frac{\partial g}{\partial q}, \frac{\partial g}{\partial \theta}\right)^T = \left(d_g, 1, -qM_g \cos 3\theta / 2\right)^T \quad (6)$$

f and *g* denote the yield and plastic potential surfaces, respectively. M_f and $d_f = (1+\alpha)(M_f - \eta)$ are model parameters. The plastic modulus during loading is defined:

$$H_L = H_0 p H_f \{H_v + H_s\} \quad (7)$$

$$H_f = \left(1 - \frac{\eta}{\eta_f}\right)^4,\ \eta_f = \left(1 + \frac{1}{\alpha}\right)M_f \quad (8a, 8b)$$

$$H_v = 1 - \frac{\eta}{M_g},\ H_s = \beta_0\beta_1 \exp(-\beta_0\xi) \quad (8c)$$

where H_L is the plastic modulus under loading; H_0 is the plastic modulus constant; H_f, H_v and H_s are plastic coefficients; η_f is the stress ratio; β_0 and β_1 are material model constants; and ξ is the accumulated plastic deviatoric strain defined as: $\xi = \int \left| d\varepsilon_s^p \right|$.

7. REFERENCES

1. de Buhan, P., and Sudret, B. "A Two phase elastoplastic model for unidirectionally reinforced materials." ***European Journal of Mechanics A/Solids***, Vol. 18, (1999), 995-1012.
2. de Buhan, P., and Sudret, B. "Micropolar multiphase model for materials reinforced by linear inclusions." ***European Journal of Mechanics A/Solids***, Vol. 19, (2000), 669-687.
3. Sudret, B., and De Buhan, P. "Multi-phase model for inclusion-reinforced geostructures Application to rock-bolted tunnels and piled raft foundations." ***International Journal of Numerical Analytical Methods Geomechanics***, Vol. 25, (2001), 155-182.
4. Hassen, G., and de Buhan, P. "A two phase model and related numerical tool for the design of soil structures reinforced by stiff linear inclusions." ***European Journal of Mechanics A/Solids***, Vol. 24, (2005), 987-1001.
5. Hassen, G., and de Buhan, P. "Elastoplastic Multi-phase model for simulating the response of piled raft foundations subject to combined loadings." ***International Journal of Numerical Analytical Methods Geomechanics***, Vol. 30, (2006), 843–864.
6. Seyedi Hosseininia, E., and Farzaneh, O. "Development and validation of a two phase model for reinforced soil by considering nonlinear behavior of matrix." ***Journal of Engineering Mechanics***, 10.1061/(ASCE)EM.1943-7889.0000111, (2009), 721–735.
7. de Buhan, P., and Hassen, G. "A multiphase model for assessing the overall yield strength of soils reinforced by linear inclusions." ***Limit State of Materials and Structures***, Springer, Dordrecht, (2013), pp: 165-178.
8. Nguyen, V. T., Hassen, G., and De Buhan, P. "Assessing the dynamic stiffness of piled-raft foundations by means of a multiphase model." ***Computers and Geotechnics***, Vol. 71, (2016), 124-135.
9. Karpurapu, R., and Bathurst, R. J. "Behaviour of geosynthetic reinforced soil retaining walls using the finite element method." ***Computers and geotechnics***, Vol. 17, No. 3, (1995), 279-299.
10. Moghadasnezhad, F. "Non Linear Finite Element Analysis of Reinforced and Unreinforeced Pavements." ***International Journal of Engineering-Transactions A: Basics***, Vol. 17, No. 3, (2004), 213-226.
11. Hatami, K., and Bathurst, R. J. "Development and verification of a numerical model for the analysis of geosynthetic-reinforced soil segmental walls under working stress conditions." ***Canadian Geotechnical Journal***, Vol. 42, No. 4, (2005), 1066-1085.
12. Qhaderi, R., Vafaeian, M., & Hashemolhoseini, H. "A parametric study of the behavior of geosynthetic reinforced soil slopes." ***International Journal of Engineering***, Vol. 18, No. 4, (2005), 371-389.
13. Hatami, K., and Bathurst, R. J. "Numerical model for reinforced soil segmental walls under surcharge loading." ***Journal of Geotechnical and Geoenvironmental Engineering***, Vol. 132, No. 6, (2006), 673-684.
14. Vafaeian, M., & Abbaszadeh, R. "Laboratory model tests to study the behavior of soil wall reinforced by weak reinforcing layers." ***International Journal of Engineering - Transactions B: Applications***, Vol. 21, No. 4, (2008), 361-374.
15. Ling, H. I., and Liu, H. "Deformation analysis of reinforced soil retaining walls—simplistic versus sophisticated finite element analyses." ***Acta Geotechnica***, Vol. 4, No. 3, (2009), 203-213.
16. Kibria, G., Hossain, M. S., and Khan, M. S. "Influence of soil reinforcement on horizontal displacement of MSE wall." ***International Journal of Geomechanics***, Vo. 14, No. 1, (2013), 130-141.

17. Shafabakhsh, G., & Motamedi, M. "Sensitivity Analysis of Road Actual Conditions to Evaluate the Optimal Positioning of Geogrid Using Finite Elements and Dynamic Methods." ***International Journal of Engineering-Transactions C: Aspects***, Vol. 29, No. 9, (2016), 1235-1241.
18. Farzaneh, O., and Iraji, A. "Two phase Model for Nonlinear Dynamic Simulation of Reinforced Soil Walls Based on a Modified Pastor-Zienkiewicz-Chan Model for Granular Soil." ***Journal of Engineering Mechanics***, Vol. 142, No. 2, (2015), 04015072.
19. Iraji, A., and Farzaneh, O. "Two phase model for nonlinear elasto-plastic behavior of reinforced soil structures using Pastor-Zienkiewicz-Chan model for matrix phase." ***Soils and Foundations***, Vol. 57, No. 6, (2017), 1014-1029.
20. Pastor, M., Zienkiewicz, O. C., and Chan, A. H. C. "Generalized plasticity and the modeling of soil behavior." ***International Journal of Numerical Analytical Methods Geomechanics,*** Vol. 14, (1990), 151–190.
21. Sudret, B. "Multiphase model for inclusion-reinforced structures" PhD Thesis, ENPC, Paris, (1999), 364 p. (in French)
22. De Buhan, P., Bourgeois, E., and Hassen, G. "Numerical simulation of bolt-supported tunnels by means of a multiphase model conceived as an improved homogenization procedure." ***International Journal of Numerical Analytical Methods Geomechanics***, Vol. 32, No. 13, (2008), 1597–1615.
23. Ling, H. I., Liu, H., and Mohri, Y. "Parametric studies on the behavior of reinforced soil retaining walls under earthquake loading." ***Journal of Engineering Mechanics***, 10.1061/(ASCE)0733-9399(2005)131:10(1056), (2005), 1056–1065.
24. Kitsabunnarat, A., Alsaleh, M., and Helwany, S. "Capturing strain localization in reinforced soils." ***Acta Geotechnica***, Vol. 3, No. 3, (2008), 175-190.
25. Zarnani, S., El-Emam, M. M., and Bathurst, R. J. "Comparison of numerical and analytical solutions for reinforced soil wall shaking table tests." ***Geomechanical Engineering***, Vol. 3, No. 4, (2011), 291–321.
26. Yang, K. H., Zornberg, J. G., Liu, C. N., and Lin, H. D. "Stress distribution and development within geosynthetic-reinforced soil slopes." ***Geosynthetics International***, Vol. 19, No. 1, (2012), 62–78.
27. Tajiri, N., Sasaki, H., Nishimura, J., Ochiai, Y., and Dobashi, K. "Full-scale failure experiments of geotextile-reinforced soil walls with different facings." Earth reinforcement H Ochiai et al., eds., Balkema, Rotterdam, The Netherlands, (1996), 525–530.
28. Berg, R. R., Christopher, B. R., and Samtani, N. C. "Design of mechanically stabilized earth walls and reinforced soil slopes"–Volume I, (2009), (No. FHWA-NHI-10-024).
29. Collin, J. G. "Design Manual for Segmental Retaining Walls." National Concrete Masonry Association, NCMA Publication No. TR 127A, (2010), 289.
30. NCMA "Design Manual for Segmental Retaining Walls, (3rd ed.)." (2009), National Concrete Masonry Association, (ed. M. Bernardi), Herndon, VA, USA.
31. PWRC "Design and Construction Manual of Geosynthetics Reinforced Soil, (revised version)." Public Works Research Center, Tsukuba, Japan, (2000), 305.

Reinforced Soil Wall Analysis under Working Stress Conditions Using a Two Phase Model with the Introduction of a New Design Parameter

A. Iraji

Engineering Faculty of Khoy, Urmia University, Urmia, Iran

P A P E R I N F O

Paper history:
Received 07 June 2019
Received in revised form 26 October 2019
Accepted 08 November 2019

Keywords:
New Design Parameter
Non-Linear Behavior
Parametric Study
Reinforced Soil Wall Displacement
Two Phase Model
Working Stress Condition

چکیده

در این تحقیق توانایی یک مدل دوفازی برای شبیه‌سازی دیوارهای خاک مسلح تحت بارهای بهره‌برداری ارزیابی شده است. این مدل دوفازی پیش از این توسط نگارنده توسعه داده شده است. مدل دوفازی یکی از روشهای همگن‌سازی بر مبنای اصل کار مجازی است. در این مدل، توده خاک مسلح از بر هم نهی دو فاز پیوسته ماتریس (خاک) و مسلح‌کننده (جوشن) تشکیل شده که در اندرکنش با همدیگر قرار دارند. با استفاده از مدل دوفازی، تغییر آرایش مسلح‌کننده‌ها و پارامترهای آنها بسیار آسانتر شده و زمان تحلیل به مقدار قابل توجهی کاهش می‌یابد. از این مدل همچنین می‌توان برای کاهش زمان لازم برای طراحی بهینه سازه‌های خاک مسلح در موارد عملی استفاده کرد. برای صحت‌سنجی مدل مذکور ابتدا نتایج پیش‌بینی مدل با یک پروژه عملی مقایسه شده است. از یک پروژه دیوار خاک مسلح ساخته شده در مقیاس بزرگ در مؤسسه پژوهشی کارهای عمومی ژاپن استفاده شده است. مدل دوفازی توسعه داده شده در یک نرم‌افزار تفاضل محدود اعمال شده و از آن برای شبیه‌سازی مدل دیوار استفاده شده است. یک مدل رفتاری الاستوپلاستیک غیرخطی برای فاز ماتریس و یک مدل رفتاری الاستیک خطی – پلاستیک کامل برای فاز مسلح‌کننده فرض شده است. سپس برای ارزیابی بیشتر و مطمئن‌تر مدل توسعه‌داده شده در ابعاد و شرایط مختلف، یک مطالعه پارامتریک گسترده شامل شبیه‌سازی ۱۲۵ مدل عددی دیوار خاک مسلح تحت شرایط بارهای بهره‌برداری انجام شده است. اثر طول، سختی و فاصله مسلح‌کننده‌ها و ارتفاع دیوار بر روی تغییرشکلهای جانبی بیشینه دیوارها بررسی شده است. در پایان یک پارامتر بی‌بعد جدید، ساده و کاربردی برای ارزیابی تغییرشکل‌های جانبی دیوارهای خاک مسلح معرفی شده است.

***doi**: 10.5829/ije.2019.32.12c.09*